Supporting Information

Fast and Stable Photochromic Oxazines

Massimiliano Tomasulo,[†] Salvatore Sortino,[*,‡] Andrew J. P. White,[§] and Françisco M. Raymo[*,†]

Center for Supramolecular Science, Department of Chemistry, University of Miami, 1301 Memorial Drive, Florida, 33146-0431, Dipartimento di Scienze Chimiche, Universitá di Catania, viale Andrea Doria 8, Catania, I-95125, Italy, and Department of Chemistry, Imperial College London, South Kensington, London, SW7 2AY, UK

E-Mail: ssortino@unict.it; fraymo@miami.edu

- General Methods and Experimental Procedures for the Synthesis of **2** and **6** S2
- High-Performance Liquid Chromatograms of **3a** and **4a** S3
- Partial ^{1}H NMR Spectra of **4a** at Various Temperatures S4
- Partial ^{1}H NMR Spectra of **3a** Before and After the Addition of Bu_4NOH S5
- Single-Crystal X-Ray Structures (ORTEP) of **3a** and **4c** S6
- Ground-State Potential Energy Profile (AM1) of **3a** S7
- Computational Data (B3LYP) for **3a**, **3b** and the transition state S8
- Steady-State Absorption Spectra of **4a** Before and After the Addition of Bu_4NOH S13
- Transient Absorption Spectra of **3a** S14
- Kinetic Trace for the Photoisomerization of **4a** S15

† University of Miami

‡ Universitá di Catania

§ Imperial College

General Methods and Experimental Procedures for the Synthesis of 2 and 6

General Methods: Chemicals were purchased from commercial sources and used as received with the exception of MeCN and CH_2Cl_2, which were distilled over CaH_2. Compound **5** was prepared according to a literature protocol.[1] The experimental procedures for the preparation of **2** and **6** are reported in the Supporting Information (Figure S1). All reactions were monitored by thin-layer chromatography, using aluminum sheets coated with silica (60, F_{254}). High-performance liquid chromatography (HPLC) was performed with analytical (column dimensions = 4.6 × 250 mm, flow rate = 1.0 mL min^{-1}, injection volume = 10 μL, sample concentration = 0.1 mM) and semi-preparative (column dimensions = 21.4 × 250 mm, flow rate = 10 mL min^{-1}, injection volume = 10 mL, sample concentration = 0.1 mM) columns. The retention time (*RT*) and the peak asymmetry (*PA*) were determined at a wavelength of 254 nm. The average purity parameter (*APP*) was calculated for the peak heart in the wavelength range 215–700 nm. Fast atom bombardment mass spectra (FABMS) were recorded in a 3-nitrobenzyl alcohol matrix.

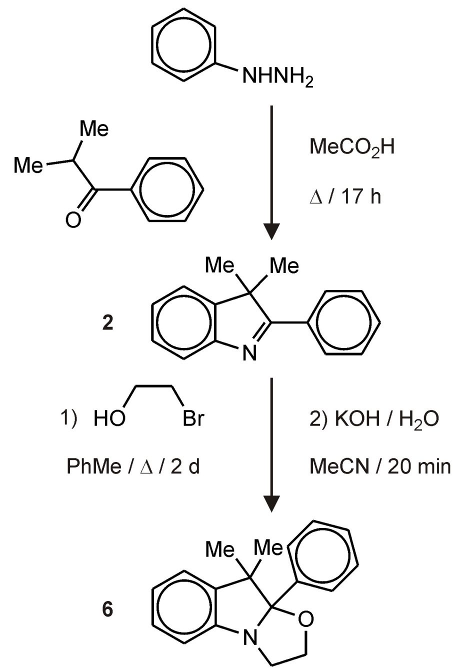

Figure S1. Synthesis of the indoline **6**.

2-Phenyl-3,3'-dimethyl-3H-indole (**2**). A solution of *i*-propylphenylketone (1.6 mL, 11 mmol) and phenylhydrazine (1.1 mL, 11 mmol) in $MeCO_2H$ (7 mL) was heated under reflux for 17 h. After cooling down to ambient temperature, the solution was diluted with H_2O (20 mL) and the pH was adjusted to *ca.* 8 with aqueous KOH (0.3 M). Then, the mixture was extracted with CH_2Cl_2 (4 × 15 mL). The organic phase was dried ($MgSO_4$), filtered and concentrated under reduced pressure to afford **2** (1.87 g, 76%) as an orange liquid. FABMS: *m/z* = 222 $[M]^+$; ^{1}H NMR (500 MHz, $CDCl_3$): δ = 1.55 (6H, s), 7.30 (1H, d, 8 Hz), 7.34–7.40 (2H, m), 7.47–7.53 (3H, m), 7.72 (1H, d, 8 Hz), 8.14–8.20 (2H, m); ^{13}C NMR (100 MHz, $CDCl_3$): δ = 24.7, 53.5, 120.7, 120.9, 126.0, 127.7, 128.3, 128.4, 128.5, 130.6, 132.9, 147.4, 183.3.

9,9-Dimethyl-9a-phenyl-2,3,9,9a-tetrahydro-oxazolo[3,2-a]indole (**6**). 2-Bromoethanol (1 mL, 28 mmol) was added to a solution of **2** (0.44 g, 2 mmol) in PhMe (25 mL) heated under reflux and Ar. The mixture was heated under reflux for a further 2 d. After cooling down to ambient temperature, the solvent was evaporated under reduced pressure. The residue was dissolved in CH_2Cl_2 (4 mL) and the solution was poured into a flask containing hexanes (35 mL) and sonicated for 30 min. The resulting precipitate was filtered off and the treatment was repeated three additional times. The solid was dissolved in a mixture of MeCN (5 mL), H_2O (10 mL) and aqueous KOH (0.3 M, 3 mL). After stirring for 20 min, the solution was concentrated under reduced pressure and extracted with CH_2Cl_2 (3 × 10 mL). The organic layer was dried ($MgSO_4$) and the solvent was evaporated under reduced pressure. The residue was purified column chromatography [SiO_2: hexanes/CH_2Cl_2 (1:1)] to afford **6** (13 mg, 3%) as a yellow solid. mp = 94°C; FABMS: *m/z* = 266 $[M + H]^+$; ^{1}H NMR (400 MHz, $CDCl_3$): δ = 0.77 (3H, s), 1.54 (3H, s), 3.30–3.34 (1H, m), 3.50–3.54 (1H, m), 3.68–3.73 (2H, m), 6.84 (1H, d, 8 Hz), 6.95–6.99 (1H, m), 7.10 (1H, d, 8 Hz), 7.18–7.23 (1H, m), 7.33–7.44 (3H, m), 7.65–7.71 (2H, m); ^{13}C NMR (100 MHz, $CDCl_3$): δ = 20.5, 29.3, 29.9, 47.8, 50.3, 63.3, 111.6, 112.1, 121.7, 122.7, 127.6, 127.8, 128.1, 138.8, 139.5, 151.2.

---

1 Raymo, F. M.; Giordani, S.; White, A. J. P.; Williams, D. J. *J. Org. Chem.* **2003**, *68*, 4158–4169.

High-Performance Liquid Chromatograms of 3a and 4a

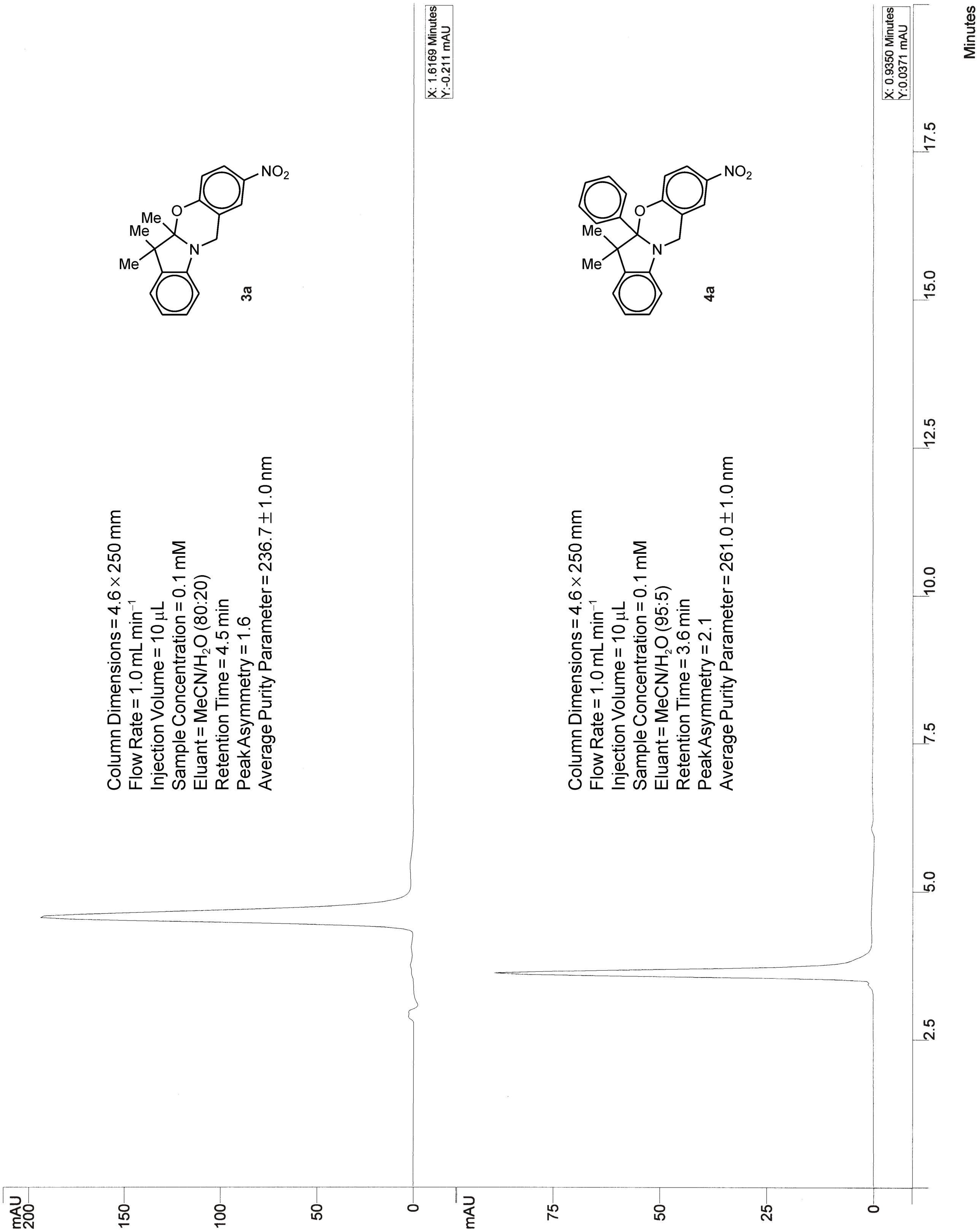

Partial [1]H NMR Spectra of 4a at Various Temperatures

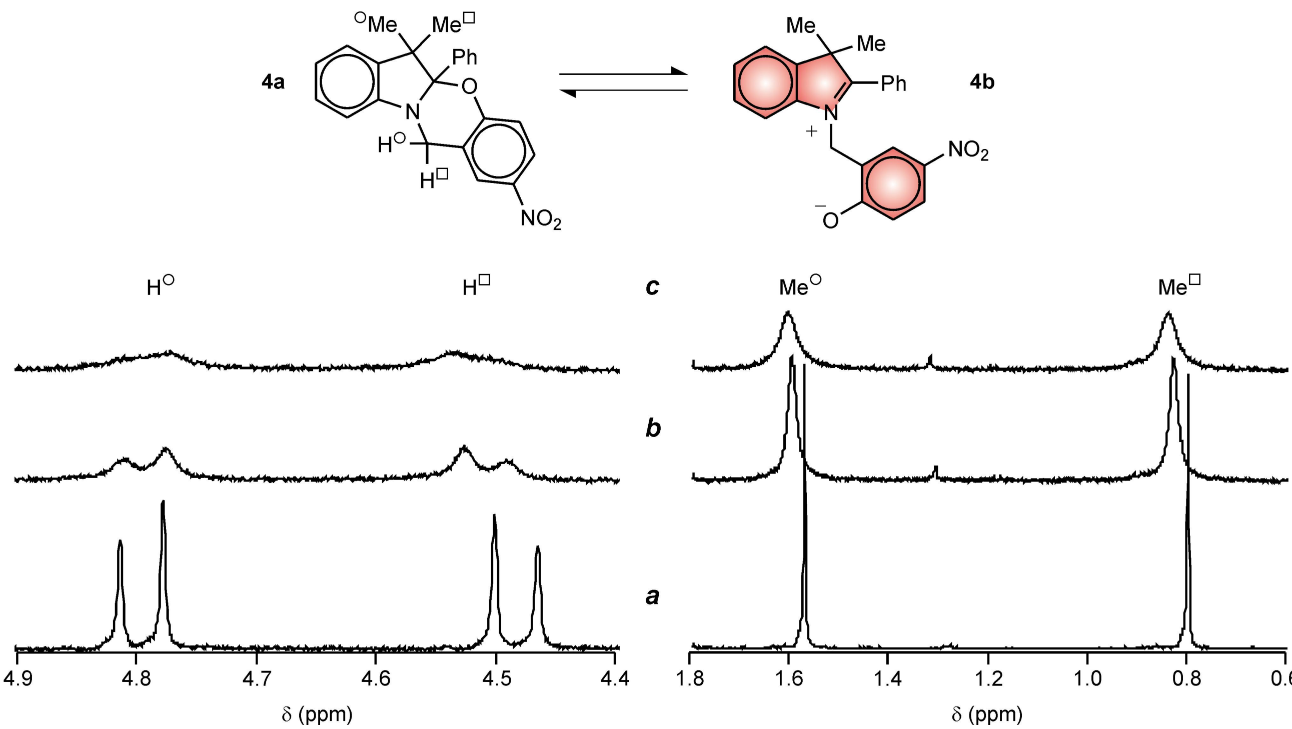

Figure S2. Partial [1]H NMR spectra (500 MHz, acetonitrile-d3, 5 mM) of **4a** at 303 (***a***), 333 (***b***) and 343 K (***c***).

Partial ^{1}H NMR Spectra of 3a Before and After the Addition of Bu_4NOH

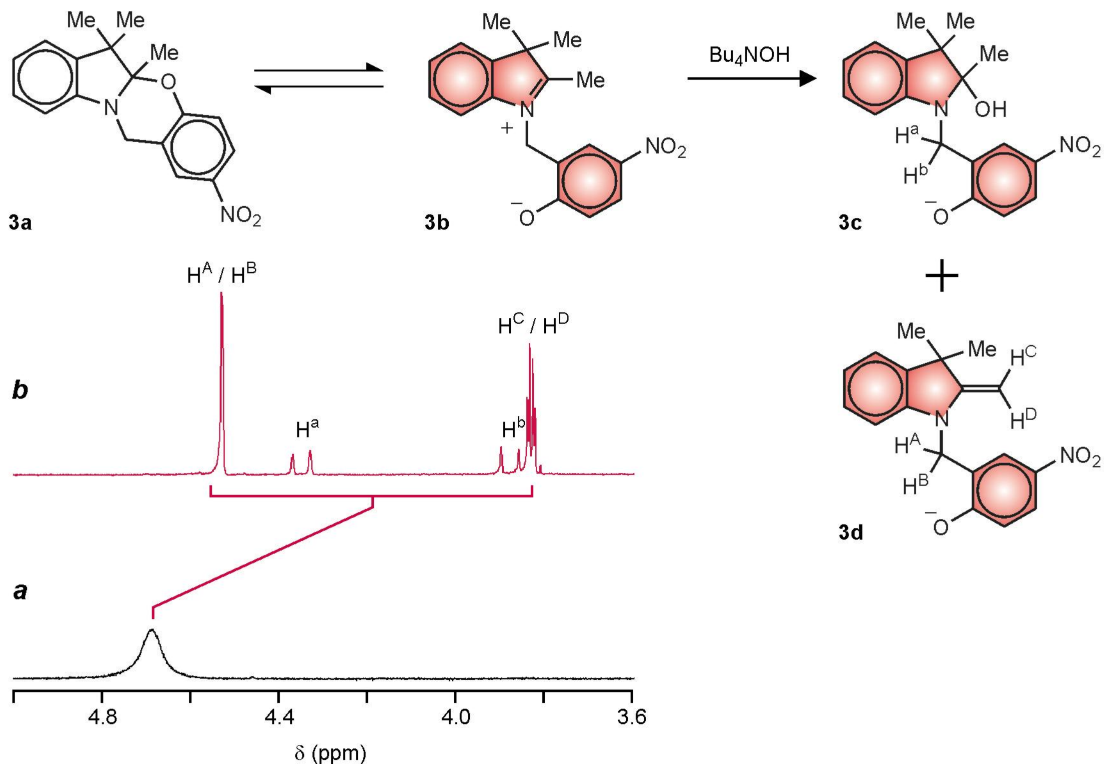

Figure S3. Partial ^{1}H NMR spectra (400 MHz, acetonitrile-d3, 10 mM) of **3a** before (***a***) and after (***b***) the addition of Bu_4NOH (2 eq.).

Single-Crystal X-Ray Structures (ORTEP) of 3a and 4c

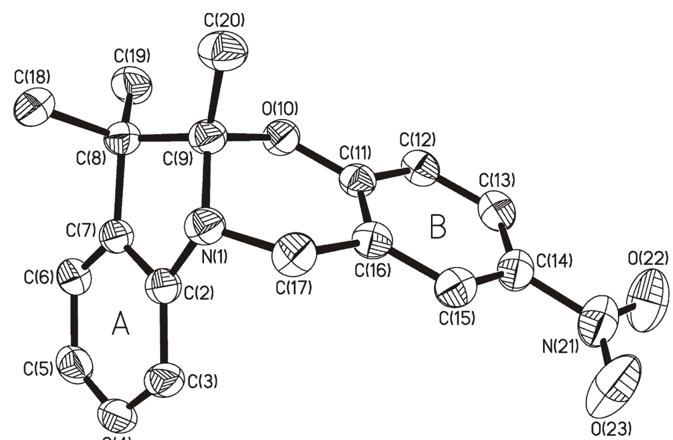

Figure S4. The single-crystal X-ray structure of **3a** (50% probability ellipsoids).

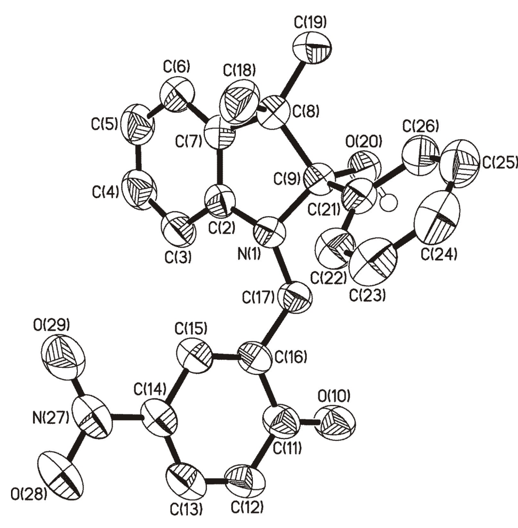

Figure S5. The single-crystal X-ray structure of **4c** (50% probability ellipsoids).

Ground-State Potential Energy Profile (AM1) of 3a

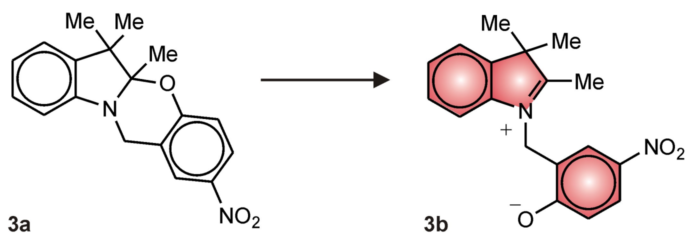

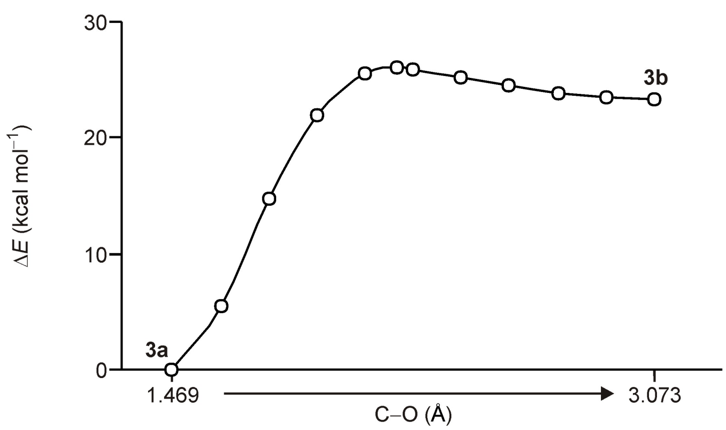

Figure S6. Energy (AM1) dependence on the C–O distance associated with the bond cleaved in the transformation of **3a** into **3b**.

Computational Data (B3LYP) for 3a, 3b and the transition state

3a

Zero-Point Corrected Energy = –1043.790847 hartrees

Number of Imaginary Frequencies = 0

Optimized Geometry:

```
 C
 C                   1        1.402515
 C                   2        1.386390    1      120.297267
 C                   3        1.402747    2      119.270999    1        -0.468500
 C                   4        1.394716    3      119.974546    2         0.437358
 C                   1        1.392327    2      121.153022    3         0.262029
 N                   1        1.415170    2      109.770008    3      -177.761053
 C                   7        1.451784    1      107.440126    2       -19.610471
 C                   2        1.523249    1      108.986085    6       177.387111
 H                   3        1.087342    2      120.576356    1      -179.936367
 H                   4        1.086056    3      119.965279    2      -179.360723
 H                   5        1.086721    4      119.768685    3      -179.798943
 H                   6        1.085800    1      121.870869    2       179.676289
 C                   9        1.547941    2      108.811538    1       -97.357889
 H                  14        1.096021    9      111.543223    2       178.831339
 H                  14        1.094709    9      109.253007    2       -62.085392
 H                  14        1.094484    9      111.600365    2        57.062283
 C                   9        1.535252    2      114.201893    1       139.959323
 H                  18        1.095669    9      109.593665    2        67.126370
 H                  18        1.096405    9      111.160682    2      -174.393152
 H                  18        1.091014    9      111.739644    2       -53.185795
 C                   7        1.458109    1      121.200860    2      -155.231136
 H                  22        1.092968    7      108.923830    1       -36.619293
 C                   8        1.524262    7      113.527985    1       158.570858
 H                  24        1.092413    8      111.021549    7       -54.288822
 C                  22        1.514414    7      111.090960    1        85.823545
 C                  26        1.410406   22      118.773581    7        17.544147
 C                  27        1.405838   26      120.428306   22      -179.051565
 C                  28        1.384804   27      120.295971   26        -0.716365
 C                  29        1.397825   28      118.932282   27         0.122882
 C                  26        1.391283   22      122.367914    7      -162.255015
 H                  28        1.084914   27      118.482489   26       179.506298
 H                  29        1.082894   28      121.536911   27      -179.767568
 H                  31        1.084681   26      120.951233   22         0.007168
 O                  27        1.353651   26      123.053501   22         0.040107
 N                  30        1.460826   29      119.406119   28      -179.970862
 O                  36        1.232966   30      117.822136   29         0.284823
 O                  36        1.233657   30      117.883852   29      -179.785382
 H                  22        1.098084    7      108.805293    1      -151.838842
 H                  24        1.094253    8      110.693621    7        66.261717
 H                  24        1.093797    8      109.951292    7      -175.125137

 1   2 1.5   6 1.5   7 1.0
 2   3 1.5   9 1.0
 3   4 1.5  10 1.0
```

```
4  5 1.5  11 1.0
5  6 1.5  12 1.0
6  13 1.0
7  8 1.0  22 1.0
8  9 1.0  24 1.0  35 1.0
9  14 1.0  18 1.0
10
11
12
13
14  15 1.0  16 1.0  17 1.0
15
16
17
18  19 1.0  20 1.0  21 1.0
19
20
21
22  23 1.0  26 1.0  39 1.0
23
24  25 1.0  40 1.0  41 1.0
25
26  27 1.5  31 1.5
27  28 1.5  35 1.0
28  29 2.0  32 1.0
29  30 1.5  33 1.0
30  31 1.5  36 1.0
31  34 1.0
32
33
34
35
36  37 1.5  38 1.5
37
38
39
40
41
```

3b

Zero-Point Corrected Energy = –1043.755388 hartrees

Number of Imaginary Frequencies = 0

Optimized Geometry:

```
C
C                   1        1.394790
C                   2        1.389174     1      119.647364
C                   3        1.399653     2      118.543350     1         0.097222
C                   4        1.398981     3      120.834638     2        -0.107278
C                   1        1.389205     2      123.042332     3        -0.000267
N                   1        1.432625     2      108.293904     3      -178.718136
C                   7        1.311877     1      110.955950     2         0.107663
C                   2        1.514903     1      108.756186     6       179.747861
H                   3        1.086591     2      121.064602     1      -179.808999
```

H	4	1.085912	3	119.594783	2	-179.837079
H	5	1.085628	4	119.747001	3	-179.487009
H	6	1.082971	1	122.229518	2	178.445019
C	9	1.546005	2	112.307439	1	-120.824785
H	14	1.094637	9	111.204735	2	175.652022
H	14	1.094578	9	109.345618	2	-65.450660
H	14	1.094676	9	111.639411	2	54.045614
C	9	1.554316	2	112.088088	1	113.690447
H	18	1.094834	9	109.170205	2	60.393658
H	18	1.094994	9	110.525269	2	179.340939
H	18	1.092652	9	110.852760	2	-60.606443
C	7	1.492599	1	122.528307	2	-167.324585
H	22	1.093949	7	107.297255	1	-59.023213
C	8	1.483743	7	124.465321	1	179.815483
H	24	1.095150	8	111.916399	7	-51.745702
C	22	1.501651	7	110.296038	1	62.986505
C	26	1.454422	22	117.765287	7	58.280975
C	27	1.443519	26	115.476661	22	179.751297
C	28	1.373842	27	122.282227	26	-0.250216
C	29	1.411649	28	120.037098	27	0.440696
C	26	1.385418	22	120.563086	7	-121.587134
H	28	1.086129	27	116.781279	26	179.954862
H	29	1.084089	28	121.493204	27	-179.748556
H	31	1.086030	26	121.582997	22	-0.385713
O	27	1.269518	26	121.725346	22	-0.946782
N	30	1.437587	29	120.242156	28	179.757412
O	36	1.239516	30	118.356946	29	0.312636
O	36	1.242678	30	118.396686	29	-179.344970
H	22	1.091605	7	106.084142	1	-174.763330
H	24	1.100279	8	106.417290	7	67.398109
H	24	1.091382	8	110.773422	7	-173.130624

```
1  2 1.5  6 1.5  7 1.0
2  3 1.5  9 1.0
3  4 1.5  10 1.0
4  5 1.5  11 1.0
5  6 1.5  12 1.0
6  13 1.0
7  8 2.0  22 1.0
8  9 1.0  24 1.0
9  14 1.0  18 1.0
10
11
12
13
14  15 1.0  16 1.0  17 1.0
15
16
17
18  19 1.0  20 1.0  21 1.0
19
20
21
22  23 1.0  26 1.0  39 1.0
23
24  25 1.0  40 1.0  41 1.0
25
26  27 1.0  31 2.0
27  28 1.5  35 2.0
```

```
28   29 2.0  32 1.0
29   30 1.5  33 1.0
30   31 1.5  36 1.0
31   34 1.0
32
33
34
35
36   37 1.5  38 1.5
37
38
39
40
41
```

Transition State

Zero-Point Corrected Energy = –1043.762001 hartrees

Number of Imaginary Frequencies = 1

Optimized Geometry:

```
C
C     1   1.394021
C     2   1.389352   1   119.657527
C     3   1.399529   2   118.611087   1      0.041402
C     4   1.398908   3   120.781672   2      0.013410
C     1   1.389503   2   122.950133   3     -0.035576
N     1   1.431079   2   108.571318   3   -179.014525
C     7   1.317727   1   110.845762   2     -1.721386
C     2   1.515242   1   108.833263   6    178.972271
H     3   1.086670   2   121.030071   1   -179.746258
H     4   1.085923   3   119.622846   2   -179.696222
H     5   1.085695   4   119.743723   3   -179.507649
H     6   1.083483   1   122.191203   2    178.513135
C     9   1.549972   2   110.901740   1   -116.373580
H    14   1.094620   9   111.278592   2    177.868966
H    14   1.094386   9   109.135080   2    -63.377432
H    14   1.094919   9   111.752493   2     55.950303
C     9   1.549306   2   113.060553   1    119.073658
H    18   1.095100   9   109.293427   2     60.189344
H    18   1.095359   9   110.379035   2    178.966690
H    18   1.091505   9   110.711787   2    -61.175463
C     7   1.490965   1   121.502340   2   -161.612381
H    22   1.093409   7   107.924605   1    -58.486682
C     8   1.487454   7   125.977559   1    175.386592
H    24   1.094584   8   109.843775   7   -134.994530
C    22   1.501723   7   108.906102   1     63.399564
C    26   1.452089  22   118.035862   7     53.162675
C    27   1.440437  26   115.833969  22   -178.948663
C    28   1.374767  27   122.145152  26     -0.851987
C    29   1.410182  28   119.946875  27      1.223026
C    26   1.385831  22   120.525809   7   -125.263830
H    28   1.086106  27   116.920064  26    179.875263
H    29   1.084005  28   121.507622  27   -179.276134
H    31   1.085863  26   121.455547  22     -1.278748
O    27   1.274357  26   121.560558  22      0.305328
N    30   1.439651  29   120.137833  28    179.430764
```

```
O               36        1.238951   30      118.310767   29        0.366831
O               36        1.241690   30      118.357184   29     -179.333373
H               22        1.091210    7      106.623787    1     -174.454736
H               24        1.090588    8      112.827610    7      -13.854669
H               24        1.094184    8      108.317531    7      105.487943

1  2 1.5  6 1.5  7 1.0
2  3 1.5  9 1.0
3  4 1.5  10 1.0
4  5 1.5  11 1.0
5  6 1.5  12 1.0
6  13 1.0
7  8 2.0  22 1.0
8  9 1.0  24 1.0
9  14 1.0  18 1.0
10
11
12
13
14  15 1.0  16 1.0  17 1.0
15
16
17
18  19 1.0  20 1.0  21 1.0
19
20
21
22  23 1.0  26 1.0  39 1.0
23
24  25 1.0  40 1.0  41 1.0
25
26  27 1.0  31 2.0
27  28 1.5  35 2.0
28  29 2.0  32 1.0
29  30 1.5  33 1.0
30  31 1.5  36 1.0
31  34 1.0
32
33
34
35
36  37 1.5  38 1.5
37
38
39
40
41
```

Steady-State Absorption Spectra of 4a Before and After the Addition of Bu_4NOH

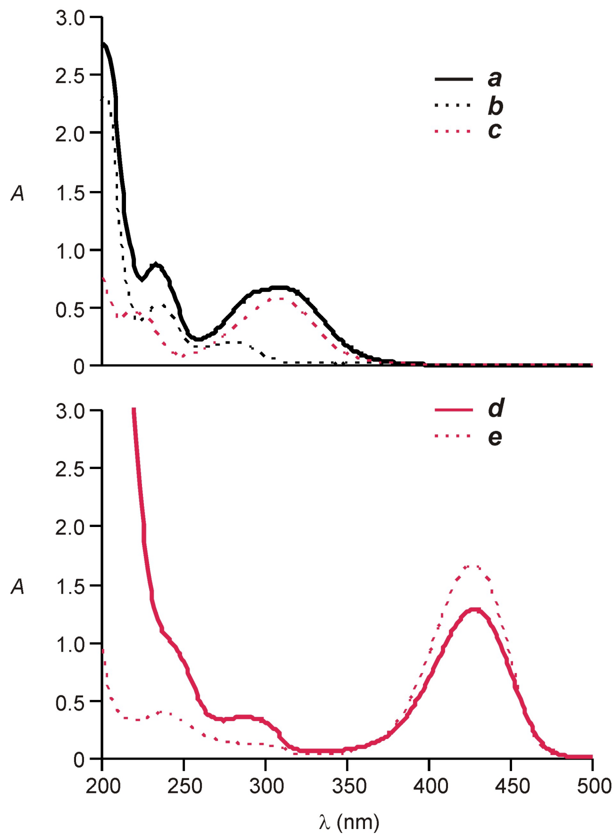

Figure S7. Steady-state absorption spectra (0.1 mM, MeCN, 298 K) of **4a** (***a***), **6** (***b***) and **7** (***c***) as well as of **4a** after the addition of Bu_4NOH (100 eq.) (***d***) and **8** (***e***).

Transient Absorption Spectra of 3a

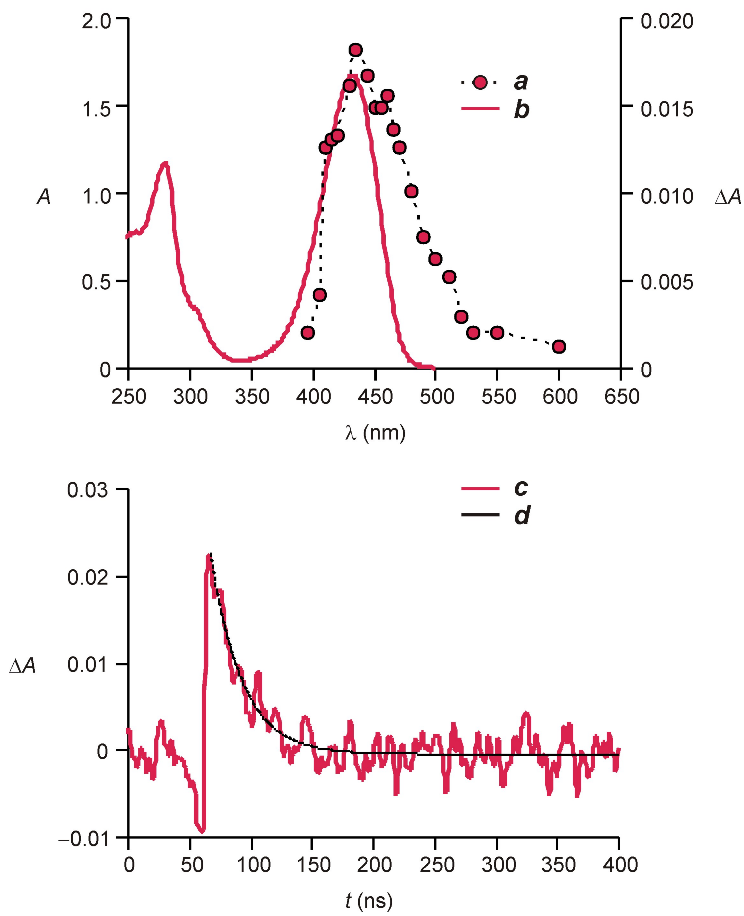

Figure S8. Transient absorption spectrum (***a***) of **3a** recorded 30 ns after the laser pulse (355 nm, 6 ns, 12 mJ, 0.1 mM, MeCN, 295 K) and steady-state absorption spectrum (***b***) of **3a** and Bu_4NOH (0.1 mM, MeCN, 298 K). Evolution of the absorbance at 440 nm (***c***) upon laser excitation of **3a** and the corresponding mono-exponential curve fitting (***d***).

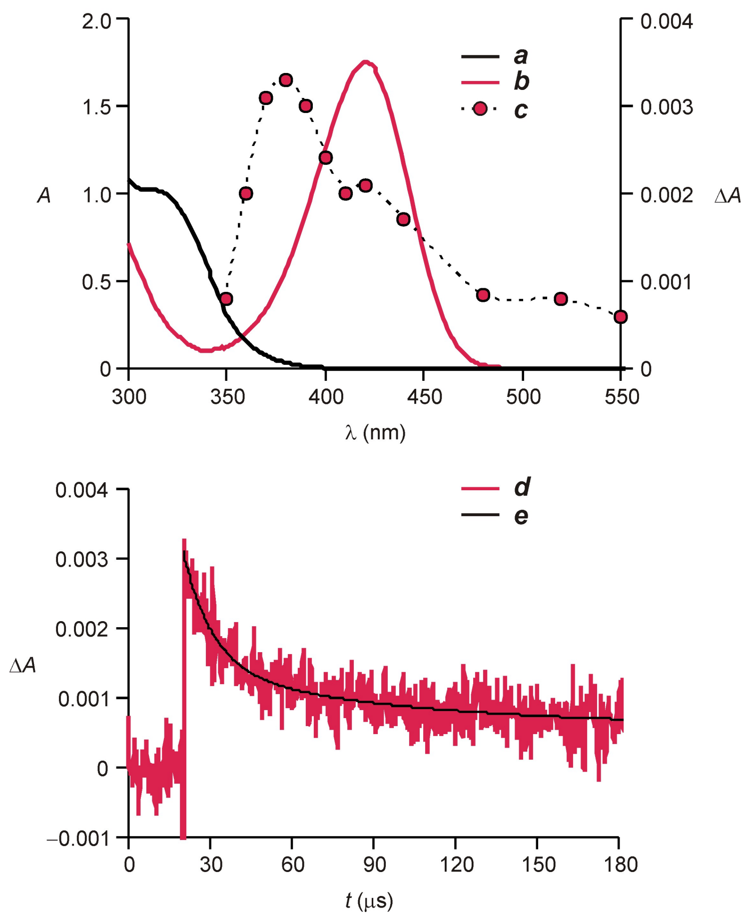

Figure S9. Steady-state absorption spectra (5%, PMMA, 298 K) of **3a** without (***a***) and with (***b***) Bu_4NOH (7 eq.) and transient absorption spectrum (***c***) of **3a** recorded 1 μs after the laser pulse (355 nm, 6 ns, 12 mJ, 5%, PMMA, 295 K). Evolution of the absorbance at 380 nm (***d***) upon laser excitation of **3a** (355 nm, 6 ns, 12 mJ, 5%, PMMA, 295 K) and the corresponding mono-exponential curve fitting (***e***).

Kinetic Trace for the Photoisomerization of 4a

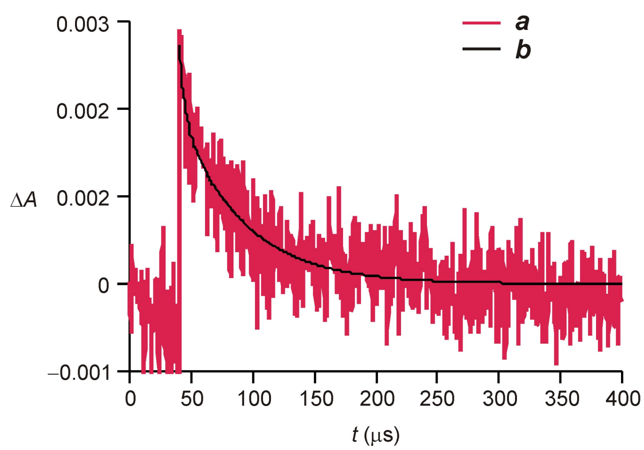

Figure S10. Evolution of the absorbance at 430 nm (***a***) upon laser excitation of **4a** (355 nm, 6 ns, 12 mJ, 5%, PMMA, 295 K) and the corresponding bi-exponential curve fitting (***b***).